

# Translocation of a single Arg<sub>9</sub> peptide across a DOPC/DOPG(4:1) model membrane using the weighted ensemble method

Seungho Choe\*

*Department of Energy Science & Engineering, Daegu Gyeongbuk Institute of Science & Technology (DGIST), Daegu 42988, South Korea and Energy Science & Engineering Research Center, Daegu Gyeongbuk Institute of Science & Technology (DGIST), Daegu 42988, South Korea*

A spontaneous translocation of cell-penetrating peptides(CPPs) in all-atom molecular dynamics(MD) simulations is not expected within a short time scale (e.g., a few hundred ns) because it is believed that the time required for the translocation of usual CPPs is on the order of minutes. In this study, we report a single Arg<sub>9</sub>(R9) peptide translocation across a DOPC/DOPG(4:1) model membrane within an order of a few tens ns scale by using the weighted ensemble(WE) method, one of the most powerful and flexible path sampling techniques. We present free energy profiles of the translocation across the membrane and identify how water molecules play a role during the translocation. We also show how the orientation of Arg<sub>9</sub> affects the translocation and how lipid molecules were transported along with Arg<sub>9</sub>. Our approach can help study interactions of CPPs with various model membranes within MD simulation approaches.

## I. INTRODUCTION

Cell-penetrating peptides(CPPs) have been extensively studied for several decades because of their capability to transport various cargoes into cells [1, 2]. Multiple factors affect the transport mechanisms of CPPs, e.g., the concentration of CPPs and the properties of the membrane [3, 4]. One of the most common difficulties in studying CPPs is that the translocation mechanisms of different CPPs are not the same, and most CPPs can have more than a single pathway depending on the experimental conditions [5].

Molecular dynamics (MD) simulations have been used to investigate functional properties of various CPPs and their interactions with many different lipids [6–8]; however, the mechanism of translocation of CPPs and interactions with lipids are still unclear within MD simulations approaches. One of the issues in MD simulations is that the spontaneous translocation of CPPs in MD simulations is not expected within a short time scale (100 ~ 200 ns) because it is believed that the time required for the translocation of CPP is on the order of minutes or so [9]. Therefore, people have been using biased simulations (e.g., umbrella sampling [10–14], steered MD simulations [15]) to study CPPs and their interactions with membranes. The umbrella sampling is very popular for obtaining a free energy barrier between CPPs and membranes. However, people have noticed that there could be an artifact in the free energy analysis.

Among various CPPs, arginine (R)-rich peptides have been extensively studied because of their effectiveness in translocation [4, 16]. Strong interaction with negatively charged phospholipid heads results in inserting R-rich peptides into the lipid bilayer. In the previous study, we implemented a weighted ensemble (WE)

method [17, 18] in all-atom MD simulations of Arg<sub>9</sub>(R9) with a DOPC/DOPG(4:1) model membrane [19]. The WE method is a very flexible path sampling technique, and it is easy to implement in any MD package. The WE method uses an ensemble of independent simulation trajectories, and each trajectory has a statistical weight. The progress coordinate is divided into bins, and trajectories are periodically replicated in bins with too few trajectories and are pruned in bins containing too many trajectories. A detailed review was given by Zuckerman and Chong [18]. We used the WESTPA software [20–22], which is widely applied to various systems, ranging from atomistic to cellular scale. One of the most significant advantages of using the WE method is that one can simulate a system without any biased potential. We found the WE method very effective for studying interactions between Arg<sub>9</sub> and the model membrane and getting free energy barriers along the penetration path. However, we couldn't find a spontaneous translocation of Arg<sub>9</sub> across the membrane because Arg<sub>9</sub> was stuck in the hydrophobic core and couldn't move for a long time [19].

In this study, the previous WE simulation [19] was continued with a few different boundaries and bin sizes, and we finally observed a spontaneous translocation of Arg<sub>9</sub> across the membrane. In the following sections, we show how a single Arg<sub>9</sub> peptide can translocate across the model membrane using the WE method and how the orientation of Arg<sub>9</sub> affects the translocation efficiency. We believe that the WE method will help study the translocation of various CPPs and their transport mechanisms.

## II. METHODS

### A. Equilibrium simulations

All simulations were performed using the NAMD package [23] and CHARMM36 force field [24]. In addi-

---

\* schoe@dgist.ac.kr

tion, we used a pre-equilibrated structure in the previous study [25], equilibrated up to 1  $\mu s$ , and was used in the previous WE simulations [19]. The detailed method regarding the WE simulations was provided in the following subsection. Here is a re-cap of equilibrium simulation: The following system was well equilibrated before starting the WE simulations: 4 Arg<sub>9</sub> with a DOPC/DOPG(4:1) membrane. CHARMM-GUI [26] was used to set up a DOPC/DOPG(4:1) membrane and TIP3P water molecules. The DOPC/DOPG(4:1) mixture consists of 76 DOPC and 19 DOPG lipids in each layer. K and Cl ions were added to each system to make a concentration of 150 mM. All Arg<sub>9</sub> peptides were initially located in the upper solution and bound to the upper layer during the equilibration. The NPT simulations were performed at T = 310K. Temperature and pressure were kept constant using Langevin dynamics. An external electric field(0.05 V/nm) was applied in the negative z-direction(from CPPs to the membrane) as suggested in previous work [7, 27] and also in our earlier simulations [19, 25] to account for the transmembrane potential [28]. The particle-mesh Ewald(PME) algorithm was used to compute the electric forces, and the SHAKE algorithm allowed a 2 fs time step during the simulation. During the equilibration, CPPs were confined in the upper water box, so there was no interaction between CPPs and the lower leaflet of model membranes. Whenever a CPP was leaving the upper water box, a small force was applied to pull that CPP inside the box. All CPPs were well contacted with the lipid molecules after the 1  $\mu s$  long equilibration, and then the WE simulations were performed using this equilibrated system.

### B. Weighted Ensemble (WE) simulations

We use the WESTPA (The Weighted Ensemble Simulation Toolkit with Parallelization and Analysis) software package [20–22] to enable the simulation of rare events, for example, translocation of CPPs across a model membrane. WESTPA is open-source, and its utility has been proven for many problems. All WE trajectories are unbiased and used to calculate conditional probabilities or transition rates.

To use the WE method in MD simulations, we need to define a progress coordinate, total number of bins, total number of walkers (child simulations) in each bin, and a time interval for splitting and combining trajectories [20]. We define the progress coordinate as a distance in the z-direction between the center of mass of phosphorus atoms in the upper leaflet and that of Arg<sub>9</sub>. After equilibration of the system, an initial distance between phosphorus atoms and Arg<sub>9</sub> was measured, and a boundary was set using this initial position and the position of the center of the membrane, for example,  $[-18 \text{ \AA}$  (the center of membrane),  $3 \text{ \AA}$  (the initial distance)]. Each bin size was 0.25  $\text{\AA}$  or 0.1  $\text{\AA}$  at different boundaries; the number of walkers in each bin was 5. Due to the short-

age of computing resources, we had to run several WE simulations to combine all the trajectories and observe the translocation of Arg<sub>9</sub> (Table I). The time interval for splitting and combining(called an iteration in Table I) the trajectories during each WE simulation was 5 ps. The total iterations during all the WE simulations were 5080. The progress coordinate was calculated using MDAnalysis [29]. The potential of mean force (PMF) profiles were obtained from each WE simulation data using “w\_pdist” and “plohist” codes in the WESTPA package [20, 21].

TABLE I: A list of WE simulations

simulation no.	bin boundaries	bin size (the smallest)	# iterations
WE1	$[-18.0 \text{ \AA}, 6.0 \text{ \AA}]$	0.25 $\text{\AA}$	664
WE2	$[-25.0 \text{ \AA}, -14.0 \text{ \AA}]$	0.25 $\text{\AA}$	3218
WE3	$[-28.0 \text{ \AA}, -21.0 \text{ \AA}]$	0.10 $\text{\AA}$	488
WE4	$[-35.0 \text{ \AA}, -25.0 \text{ \AA}]$	0.10 $\text{\AA}$	514
WE5	$[-45.0 \text{ \AA}, -33.0 \text{ \AA}]$	0.10 $\text{\AA}$	196

## III. RESULTS

### A. Translocation of a single Arg<sub>9</sub> peptide was observed within a very short time scale

We observe that a single Arg<sub>9</sub> translocates the model membrane during the WE simulations. In the previous WE simulation, the translocation of Arg<sub>9</sub> was not observed because Arg<sub>9</sub> was trapped in a hydrophobic core for a long time [19]. In the current simulations, the size of each bin was decreased from 0.25  $\text{\AA}$  in the previous WE simulation [19] to 0.10  $\text{\AA}$ , which could help Arg<sub>9</sub> overcome potential energy barriers along the translocation path. Hereafter, Arg<sub>9</sub> represents the single peptide that implemented the WE method if there is no specific explanation. The other three Arg<sub>9</sub> peptides were closely contacted with the upper leaflet during the simulations, and they didn’t show any translocation or any meaningful penetration.

Fig. 1 shows the penetration depth of both Arg<sub>9</sub> vs. the number of iterations of WE simulations. Here, an iteration means splitting-combining trajectories at every 5 ps. We define the penetration depth as the distance between the center of mass of CPP and that of the upper leaflet’s phosphorus(P) atoms. Therefore, the negative sign denotes that Arg<sub>9</sub> is located below the upper leaflet. The maximum penetration depth of Arg<sub>9</sub> in the previous WE simulation was about  $-17.6 \text{ \AA}$  [19], and now it can reach up to  $-45 \text{ \AA}$  in the current simulations.

As shown in the figure, the penetration depth changes rapidly within a very short time scale. As described in the Methods section, each iteration corresponds to 5 ps long, and the figure shows that Arg<sub>9</sub> can translocate the model membrane within a very short time ( $\sim 25$  ns) since

the WE simulation started. Therefore, the WE method provides a very effective tool to overcome potential energy barriers between Arg<sub>9</sub> and the model membrane. Thus the WE method could be used to study interactions between membrane-active peptides(MAPs), including cell-penetrating peptides(CPPs) and antimicrobial peptides(AMPs), and various model membranes within MD simulation approaches.

Fig. 2 presents snapshots of Arg<sub>9</sub> during the WE simulations. They are snapshots at the 1500th, 3000th, 4500th, and the last iteration. We have 5080 iterations from WE1 to WE5 simulations. In the figure, yellow shows Arg<sub>9</sub>, and gray is the lipid molecules in the model membrane (DOPC/DOPG(4:1)). The blue and red dots are phosphorus atoms of the upper and the lower leaflets, respectively. Water molecules, ions, and the other three Arg<sub>9</sub>s are omitted for clarity. As shown in Fig. 2, the membrane is deformed when Arg<sub>9</sub> penetrates the middle of the membrane. There are two interesting findings during the deformation of the model membrane: The first finding is that a part of the lipids in the upper leaflet moved along with Arg<sub>9</sub>. The last iteration showed that these lipids went through the lower leaflet. Later, we will discuss how these lipids are transported and reorganized in the model membrane. The second finding is the disruption of the lower leaflet both at 4500th and at the last iteration shown in the figure. When Arg<sub>9</sub> comes to the bottom of the membrane, the lower leaflet deforms drastically, and it makes a widening of a water pore in the lower leaflet.

During the translocation, one of the interesting quantities would be hydrogen bonds between Arg<sub>9</sub> and the lipids molecules. It has been known that the hydrogen bonding between CPPs and lipids (or water) is critical when CPPs contact the membrane at the beginning of the penetration and make the translocation across the membrane [30–33]. Fig. S1 presents the number of hydrogen bonds during the translocation (from WE1 to WE5 simulations). The blue line denotes the number of hydrogen bonds between Arg<sub>9</sub> and the lipid molecules, while the green is between Arg<sub>9</sub> and the phosphate group in the lipids. The red line depicts the ones between Arg<sub>9</sub> and water. Each point in the figure is an averaged value over 10 iterations. The average number of hydrogen bonds between Arg<sub>9</sub> and the lipids (or water) is about 20, and this number showed a slight fluctuation during the translocation. This indicates that the strength of hydrogen bonding doesn't affect the efficiency of the translocation. Although the hydrogen bonding between Arg<sub>9</sub> and the membrane is vital at the initial penetration stage, our simulation suggests that another factor could be responsible for translocating Arg<sub>9</sub> across the membrane. We think that water can be one factor that makes the translocation which we will discuss in the following section.

Another attractive quantity is the conformational change during the translocation. It has been known that Arg<sub>9</sub> stayed at a random coil both in the solution and in the membrane environment [34]. Fig. S2 shows the con-

formational change of four Arg<sub>9</sub>s during the WE simulation, identified using the Timeline in VMD [35]. The red box corresponds to Arg<sub>9</sub>, which showed the translocation across the membrane, while the other three didn't show the translocation. During the translocation (Arg<sub>9</sub> in the red box), most arginine residues showed a turn(aqua) in the Timeline graph, and this structure remained until the end of the simulation. The other three Arg<sub>9</sub>s showed a random coil(white) or a combination of both a coil and a turn, and this is because most parts of Arg<sub>9</sub>s were exposed to water molecules in the upper solution. Our simulation suggests a distinct conformational change (from a random coil to a turn) when Arg<sub>9</sub> translocates across the membrane.

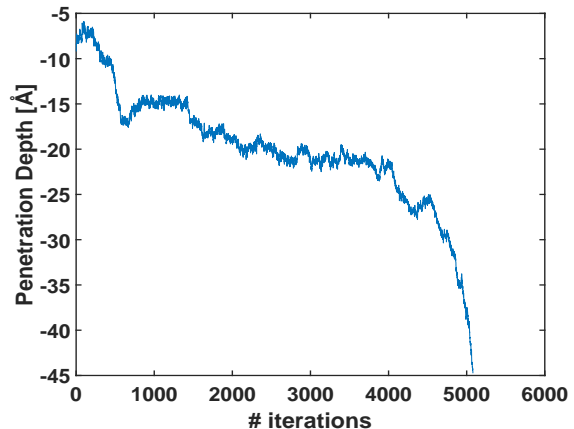


FIG. 1: The penetration depth vs. the number of iterations, where an iteration denotes splitting-combining trajectories. Each iteration takes 5 ps in our WE simulation.

### B. Water molecules play a role in translocating Arg<sub>9</sub> across the model membrane

The pore formation process has been well known based on MD simulations of one of the antimicrobial peptides, melittin [36]. According to their results, a P/L(peptide/lipid) ratio and aggregation of peptides were necessary for making pores. Although we didn't see the aggregation of Arg<sub>9</sub>s, our simulation suggests that even a single Arg<sub>9</sub> can induce a water pore.

When Arg<sub>9</sub> approaches the middle of the model membrane, the number of water molecules coordinated with Arg<sub>9</sub> increases, as shown in Fig. 3. A water pore is shown at the 4500th iteration; however, most of the pore is blocked by Arg<sub>9</sub>. Only a few water molecules can translocate across the membrane. Fig. 4 presents the total accumulated number of water molecules translocated across the membrane (up & down) as a function of time.

We counted a number of water molecules that translocate across the membrane from  $z = +10 \text{ \AA}$  to  $z =$

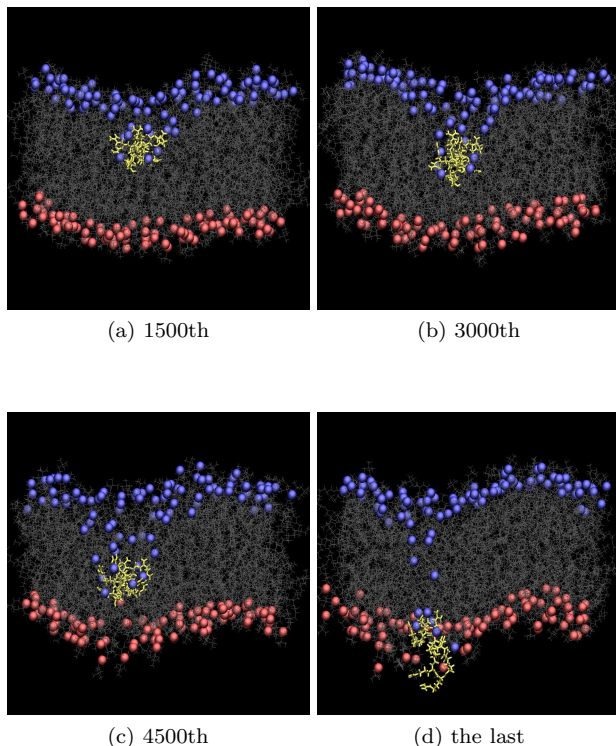


FIG. 2: Snapshots at (a) 1500th (b) 3000th (c) 4500th, and (d) the last iteration. (yellow: Arg<sub>9</sub>, grey: lipids, blue & red : phosphorus atoms of the upper leaflet & lower leaflet, respectively)

$-10 \text{ \AA}$  as the moving-down, and water molecules from  $z = -10 \text{ \AA}$  to  $z = +10 \text{ \AA}$  as the moving-up. It is interesting to see an increase in the moving-down water molecules when Arg<sub>9</sub> approaches the bottom of the membrane. On the other hand, the number of the moving-up water molecules has slightly changed during the last part of the simulation. Therefore, there is a strong correlation between the direction of water flow and the movement of Arg<sub>9</sub>. The rapid increase in the number of downward water molecules is closely related to the orientation of Arg<sub>9</sub> to the membrane, as shown in the following section.

During the WE simulation, the downward water flux was about 5.9 (water molecules/ns), while the upward water flux was 1.6. If we count only the number of water molecules during the last part of translocation after the water pore was made, the downward water flux was 44.8 (water molecules/ns), and the upward water flux was 12.4. These numbers can be compared with the previous result ( $6.2 \sim 27.3$ ), where the water pore was made by moving a single lipid to the center of the bilayer using the umbrella sampling [37]. It turns out that the water pore is very transient in our WE simulations, and it is closed soon after Arg<sub>9</sub> is translocated to the bottom of the membrane. We will discuss more on the closure of the water pore in one of the following sections.

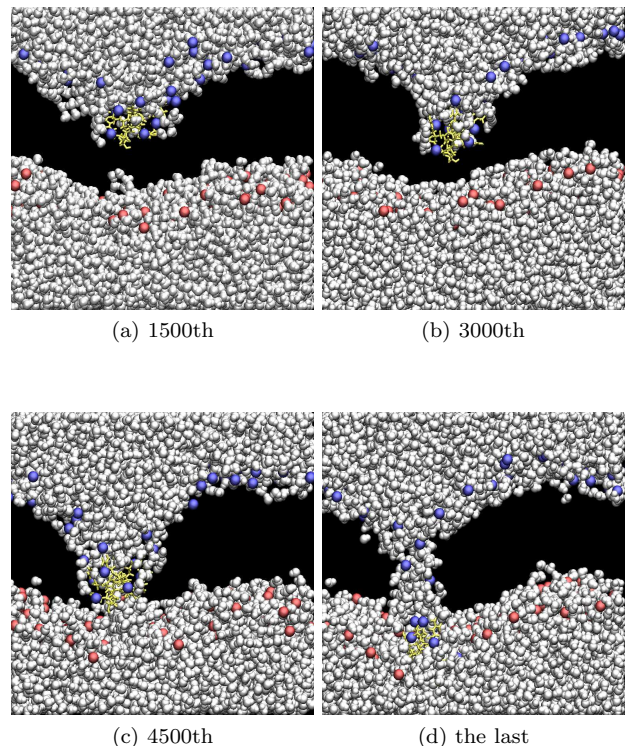


FIG. 3: Water molecules coordinated with Arg<sub>9</sub> at (a) 1500th (b) 3000th (c) 4500th, and (d) the last iteration. (yellow: Arg<sub>9</sub>, white: water, blue & red : phosphorus atoms of the upper leaflet & lower leaflet, respectively)

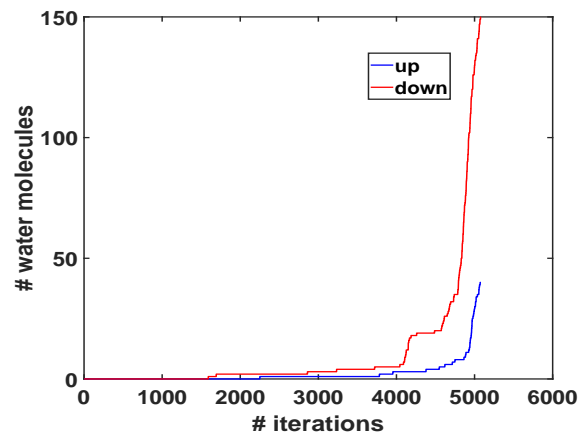


FIG. 4: A total number of water molecules translocated across the membrane (the moving-up & the moving-down) vs. the number of iterations

### C. The orientation angle of Arg<sub>9</sub> affects the translocation

As shown in Fig. 1, the penetration depth was increased rapidly during the last part of the translocation (4500th  $\sim$ ). In the previous section, we mentioned that

the rapid penetration is related to the water flow. In this section, we show that the orientation angle of an Arg<sub>9</sub> peptide also affects the efficiency of the translocation.

We define the orientation angle of the peptide as follows: First, obtain the center of mass positions of the first three and the last three Ca's of Arg<sub>9</sub>. Second, find a vector( $\vec{v}_1$ ) connecting those two center-of-mass positions. Last, calculate an angle between the vector  $\vec{v}_1$  and a unit vector parallel to the z-axis (e.g.,  $\vec{v}_2 = (0,0,1)$ ). Thus, a smaller angle means that the peptide is almost normal to the model membrane. Note that the conformation of Arg<sub>9</sub> is a random coil both in solution and in the membrane environment [34], and our simulation shows a turn during the translocation (Fig. S2). Therefore, the calculated angle is not as precise as in the case of a straight helix; however, our calculation will give us an idea of how Arg<sub>9</sub> is oriented during the translocation. Fig. 5 shows the orientation angle of Arg<sub>9</sub> during the translocation. During most simulation time, Arg<sub>9</sub> is almost parallel to the surface of the model membrane ( $70^\circ \sim 90^\circ$ ); however, the orientation is rapidly changed to a smaller angle ( $\sim 40^\circ$ ) when the peptide reaches the bottom of the model membrane. Based on this figure, one can conjecture that Arg<sub>9</sub> with a smaller orientation angle shows more efficient translocation across the model membrane. This efficiency should be related to potential energy barriers between Arg<sub>9</sub> and the model membrane.

Fig. 6 shows the potential of mean force (pmf) along the translocation path of Arg<sub>9</sub>. The WESTPA package provides the free energy based on the WE simulation data without applying any biased potential [20]. We have obtained five pmf profiles (Fig. S3) from five WE simulations (WE1 ~ WE5) at different bin boundaries and combined them to connect to each other. One can compare the slope of each free energy in Fig. 6. When Arg<sub>9</sub> approaches the bottom of the membrane (e.g., the WE4 & WE5 simulations), the potential energy barrier decreases compared with those in the hydrophobic core (e.g., the WE2 & WE3 simulations). During the WE4 & WE5 simulations, the penetration depth is drastically increased, and the number of transported water molecules increases. Our simulation confirms the previous simulations [8, 38] that the potential energy barrier becomes lower in the presence of the water pore. The total free energy barrier from the upper solution to the bottom of the lower leaflet is about 1,000 kT. The translocation of single Arg<sub>9</sub> across the DOPC/DOPG(4:1) membrane is energetically unfavorable even though the water molecules decrease the energy barrier.

As shown in Table S1, there are two additional simulations at  $[-45.0 \text{ \AA}, -33.0 \text{ \AA}]$ , i.e., WE5a and WE5b simulations. We want to compare the pmf plot and the orientation angle of Arg<sub>9</sub> in each simulation. In Fig. S4, we compare the penetration depth and the orientation angle from WE5, WE5a, and WE5b simulations. The solid blue and red lines correspond to the penetration depth and orientation angle from the WE5 simulation. The results from the WE5a and WE5b simulations were

shown as the dashed and dashed-dot lines in the figure. When the penetration depth changes rapidly, the orientation angle shows similar behavior. Whenever Arg<sub>9</sub> reaches the bottom of the membrane, the orientation angle becomes smaller ( $40 \sim 50^\circ$ ). The upright position seems energetically favorable for translocation of Arg<sub>9</sub> in our simulation. In Fig. S5, WE5a and WE5b simulations show higher potential energy barriers than the WE5 simulation due to the orientation of Arg<sub>9</sub> during the translocation. Our simulation suggests that the water flow and the orientation angle of Arg<sub>9</sub> are essential for translocation.

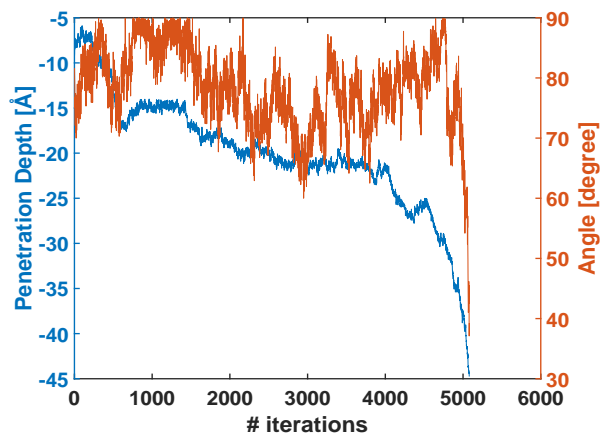


FIG. 5: The penetration depth (blue line) and the orientation angle (red line) of Arg<sub>9</sub> vs. the number of iterations.

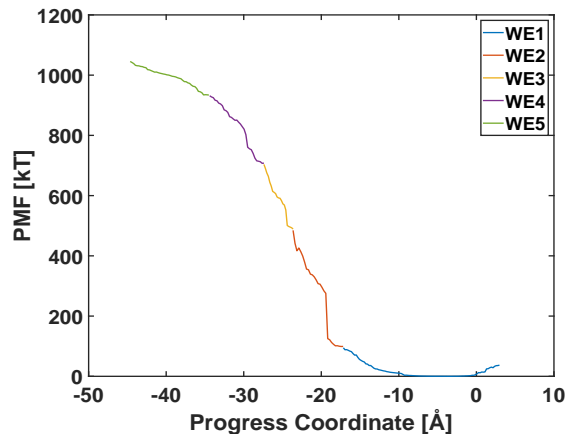


FIG. 6: The potential of mean force (pmf) vs. the progress coordinate.

#### D. The water pore was very transient and lipid flip-flops were observed

When Arg<sub>9</sub> was located at the bottom of the membrane, the WE5 simulation was stopped, and an additional equilibrium simulation (without using the WE method) was run at this position. The equilibrium simulation method is the same as in the Methods section and in the previous work [19, 25]. A total of 1  $\mu$ s equilibrium simulation was performed. During the equilibrium simulation, Arg<sub>9</sub> moved up and down for a while, and eventually, it moved to the bottom of the membrane and stayed there until the end of the simulation. The water pore was closed at 70 ns, and there was no translocation of water molecules after that. Fig. S6 presents several snapshots during this equilibrium simulation which show a closure of the water pore and the behavior of Arg<sub>9</sub>. The pore lifetime in our simulations (WE simulations + an additional equilibrium simulation) is less than 100 ns (Fig. S7), and the order of lifetime is very similar to the previous results [39, 40].

Another interesting finding during the equilibrium simulation was translocation of lipids molecules. The phospholipids(PL) flip-flop (or PL translocation) has been well studied in numerous works [11, 41–48]. There are two primary mechanisms for the lipid flip-flop: One is water pore-mediated. The other one is peptide-mediated. As shown in Fig. 2, a few lipids in the upper leaflet moved down along with Arg<sub>9</sub>. A total of six DOPG lipids moved down to the lower leaflet during the WE simulation, and two of them moved back to the upper leaflet when Arg<sub>9</sub> moved up during the equilibrium simulation (Fig. S6). Our simulation shows that the lipids' location was switched rapidly from the upper leaflet to the lower leaflet and vice versa. The total time of PL translocation (moved from the upper leaflet to the lower and then moved back to the upper leaflet) was about 75 ns. This time scale is due to the fast movement of Arg<sub>9</sub> in our simulations. Our simulations suggest that the primary mechanism of the lipid translocation is a peptide-mediated process; however, the water flow also affects PL translocation because the peptide movement and the water flow are closely related as shown both in the WE simulations and the additional equilibrium simulation. We found that the translocated lipids were quickly reorganized (Fig. S6). After the translocation of lipids to the lower or the upper leaflet, the flip-flopped lipids were well reorganized with the other lipids during the equilibrium simulation.

## IV. DISCUSSION

Translocation of a single Arg<sub>9</sub> was observed using the WE method within the MD simulations approach. Compared with the previous WE simulation [19], which didn't show any translocation of Arg<sub>9</sub> across the membrane, the smaller bin size is one of the critical factors in making a

spontaneous translocation across the model membrane. Finding an appropriate number of walkers and a reasonable bin size in the WE simulations is difficult without any trial and error. Note that an adaptive bin scheme was already developed for the WE simulation to change the bin size on-the-fly [49]. This scheme could be applied to the current work to make rapid translocation of Arg<sub>9</sub> or any other CPPs to study their transport mechanisms. Our WE simulations showed that translocation of a single Arg<sub>9</sub> was energetically unfavorable due to much higher potential energy barriers ( $\sim 1,000$  kT) between Arg<sub>9</sub> and the model membrane along the translocation path compared with the previous calculation ( $\sim 100$  kT) from the upper solution to the center of the membrane [19].

It has been known that one of the essential factors in the translocation of CPPs is a concentration of peptides. Although we used four Arg<sub>9</sub>s in our WE simulation, the concentration in a local area is not enough to see collective behavior between Arg<sub>9</sub>s. The progress coordinate in our WE simulation was defined as a distance between the upper leaflet and one of the Arg<sub>9</sub>s, and thus the other three Arg<sub>9</sub>s didn't show any penetration into the model membrane during the whole simulation. The collective behavior between CPPs could enhance the efficiency of translocation. Although our simulation shows that translocation of a single CPP is not favorable, the WE method can be used to study spontaneous translocation at low concentration. One can implement a progress coordinate as a distance between the center of mass of the upper leaflet's phosphorus atoms and more than two CPPs, e.g., two Arg<sub>9</sub>s, three Arg<sub>9</sub>s, or four Arg<sub>9</sub>s at the same time. However, our experience in the WE simulations shows that it is not easy to observe simultaneous translocation of more than two CPPs due to much slower CPPs than a single CPP movement.

Another critical factor in our successful translocation is the orientation of Arg<sub>9</sub> relative to the membrane. Our simulation showed that the orientation angle of Arg<sub>9</sub> is vital to determining the free energy barrier along the translocation path of Arg<sub>9</sub>. It is much easier for Arg<sub>9</sub>, which was located normal to the membrane (i.e., parallel to the z-axis), to translocate across the membrane, as shown in the free energy analysis (Fig. S5). It has been known that the orientation of peptides is dependent on the concentration. For example, a two-state model has been suggested for the orientation of adsorbed peptides: S-state & I-state [50]. Here, the S-state means that peptides are parallel to the membrane and observed at low P/L's, while the I-state denotes that peptides are perpendicular to the membrane and observed above the threshold concentration. To stabilize the water pore, it is necessary to change the average peptide orientation from S to I [11, 50]. The threshold value (P/L\*) is the peptide concentration when the energy levels of the S state and the I state are equal. Although Huang's two-state model was initially developed for antimicrobial peptides, the orientation of Arg<sub>9</sub> relative to the membrane in our

simulations can also be dependent on the P/L ratio. The P/L ratio in our system is low ( $P/L \sim 0.042$ ); however, this ratio is much greater than the critical thresholds in the literature [11, 51]. Note that the threshold value ( $P/L^*$ ) varies with the lipid composition of the membrane [11, 50, 51]. Arg<sub>9</sub> stayed at the S state during most of the simulation time and turned into the I state during the last part of the simulation. Although we found the translocation of Arg<sub>9</sub> across the model membrane within a very short time (a few tens ns), it is necessary to work on different lipid compositions and concentrations to see if there is any significant change in this time scale.

Based on our observation of the spontaneous translocation of Arg<sub>9</sub>, it is very promising that the WE method can be applied to any membrane-active peptides (MAPs), including both CPPs and AMPs, which we need the in-

formation on interactions between peptides and various membranes, and on transport mechanisms as well. We expect the WE method to provide a very effective way to study protein-lipid interactions within MD simulation approaches.

## ACKNOWLEDGMENTS

This work was supported by the Faculty start-up fund from DGIST and the DGIST R&D Program of the Ministry of Science and ICT (22-BRP-12). In addition, the author would like to thank the DGIST Supercomputing Big Data Center for computing resources and the National Supercomputing Center for supercomputing resources, including technical support (KSC-2021-CRE-0296).

- 
- [1] G. Guidotti, L. Brambilla, and D. Rossi, *Trends in Pharmacological Sciences* **38**, 406 (2017).
- [2] A. Walrant, S. Cardon, F. Burlina, and S. Sagan, *Accounts Chem Res.* **50**, 29682975 (2017).
- [3] M. D. Pisa, G. Chassaing, and J. Swiecicki, *Biochemistry* **54**, 194 (2015).
- [4] I. Ruseska and A. Zimmer, *Beilstein J. of Nanotechnol.* **11**, 101 (2020).
- [5] F. Madani, S. Lindberg, . Langel, S. Futaki, and A. Gräslund, *J. Biophys.* **2011**, 1 (2011).
- [6] H. D. Herce and A. E. Garcia, *Proc. Natl. Acad. Sci. USA* **104**, 20805 (2007).
- [7] H. D. Herce, A. E. Garcia, J. Litt, R. S. Kane, P. Martin, N. Enrique, A. Rebolledo, and V. Milesi, *Biophys. J.* **97**, 1917 (2009).
- [8] S. Yesylevskyy, S.-J. Marrink, and A. Mark, *Biophys. J.* **97**, 40 (2009).
- [9] M. Zorko and Ü. Langel, *Adv. Drug Deliv. Rev.* **57**, 529 (2005).
- [10] M. Pourmousa, J. Wong-ekkabut, M. Patra, and M. Karttunen, *J. Phys. Chem. B* **117**, 230 (2013).
- [11] D. Sun, J. Forsman, M. Lund, and C. E. Woodward, *Phys.Chem.Chem.Phys.* **16**, 20785 (2014).
- [12] G. Teseia, M. Vazdarb, M. R. Jensenc, C. Cragnella, P. E. Masond, J. Heydae, M. Skepo, P. Jungwirthd, and M. Lunda, *PNAS* **114**, 11428 (2017).
- [13] C. Yao, Z. Kang, B. Yu, Q. Chen, Y. Liu, and Q. Wang, *Langmuir* **35**, 92869296 (2019).
- [14] F. H. Choong and B. K. Yap, *ChemPhysChem* **22**, 493 (2021).
- [15] M. J. Akhunzada, B. Chandramouli, N. Bhattacharjee, S. Macchi, F. Cardarelli, and G. Brancato, *Phys. Chem. Chem. Phys.* **19**, 27603 (2017).
- [16] M. M. Fretz, N. A. Penning, S. Al-Taei, S. Futaki, T. Takeuchi, I. Nakase, G. Storm, and A. T. Jones, *Biochem. J.* **403**, 335 (2007).
- [17] G. Huber and S. Kim, *Biophys J.* **70**, 97110 (1996).
- [18] D. M. Zuckerman and L. T. Chong, *Annu. Rev. Biophys.* **46**, 43 (2017).
- [19] S. Choe, *Membranes* **11**, 974 (2021).
- [20] M. C. Zwier, J. L. Adelman, J. W. Kaus, A. J. Pratt, K. F. Wong, N. B. Rego, E. Suarez, S. Lettieri, D. W. Wang, M. Grabe, D. M. Zuckerman, and L. T. Chong, *J. Chem. Theory Comput.* **11**, 800 (2015).
- [21] A. T. Bogetti, B. Mostolan, A. Dickson, A. Pratt, A. S. Saglam, P. O. Harrison, J. L. Adelman, M. Dudek, P. A. Torrillo, A. J. DeGrave, U. Adhikari, M. C. Zwier, D. M. Zuckerman, and L. T. Chong, *Living J. Comp. Mol. Sci.* **1**, 10607 (2019).
- [22] J. Russo, S. Zhang, J. Leung, A. Bogetti, J. Thompson, A. DeGrave, P. Torrillo, A. Pratt, K. Wong, J. Xia, J. Copperman, J. Adelman, M. Zwier, D. LeBard, D. Zuckerman, and L. Chong, *J Chem Theory Comput.* **18**, 638649 (2022).
- [23] J. Phillips, R. Braun, W. Wang, J. Gumbart, E. Tajkhorshid, E. Villa, C. Chipot, R. D. Skeel, L. Kale, and K. Schulten, *J. Comput. Chem.* **26**, 1781 (2005).
- [24] B. R. Brooks, C. L. B. III, A. D. M. Jr., L. Nilsson, R. J. Petrella, B. Roux, Y. Won, G. Archontis, C. Bartels, S. Boresch, and et al, *J. Comput. Chem.* **30**, 1545 (2009).
- [25] S. Choe, *AIP Advances* **10**, 105103 (2020).
- [26] S. Jo, T. Kim, V. G. Iyer, and W. Im, *J. Comput. Chem.* **29**, 1859 (2008).
- [27] A. Walrant, A. Vogel, I. Correia, O. Lequin, B. E. S. Olausson, B. Desbat, S. Sagan, and I. D. Alves, *Biochimica Biophysica Acta* **1818**, 1755 (2012).
- [28] B. Roux, *Biophys. J.* **95**, 4205 (2008).
- [29] N. Michaud-Agrawal, E. J. Denning, T. B. Woolf, and O. Beckstein, *J. Comput. Chem.* **32**, 2319 (2011).
- [30] J. Rothbard, T. Jessop, R. Lewis, B. Murray, and P. Wender, *J Am Chem Soc* **126**, 95069507 (2004).
- [31] M. Tang, A. Waring, R. Lehrer, and M. Hong, *Angewandte Chemie Int Ed.* **47**, 32023205 (2008).
- [32] Y. Takechi-Haraya and H. Saito, *Current Protein and Peptide Science* **19**, 623 (2018).
- [33] D. Pei, *Accounts Chem Res* **55**, 309 (2022).
- [34] E. Eiríksdóttir, K. Konate, Ü. Langel, G. Divita, and S. Deshayes, *Biochimica Biophysica Acta* **1798**, 1119 (2010).
- [35] W. Humphrey, A. Dalke, and K. Schulten, *J. Molec. Graphics* **14**, 33 (1996).
- [36] D. Sengupta, H. Leontiadou, A. E. Mark, and S.-J. Mar-

- rink, *Biochimica et Biophysica Acta* **1778**, 2308 (2008).
- [37] W. F. D. Bennett, N. Sapay, and D. P. Tieleman, *Biophys. J.* **106**, 210 (2014).
- [38] K. Huang and A. E. Garcia, *Biophys. J.* **104**, 412 (2013).
- [39] S. Marrink, E. Lindahl, O. Edholm, and A. Mark, *J Am Chem Soc.* **123**, 86388639 (2001).
- [40] A. de Vries, A. Mark, and S. Marrink, *J Am Chem Soc.* **126**, 44884489 (2004).
- [41] E. Fattal, S. Nir, R. A. Parente, and J. F. C. Szoka, *Biochemistry* **33**, 6721 (1994).
- [42] K. Matsuzaki, O. Murase, N. Fujii, and K. Miyajima, *Biochemistry* **35**, 11361 (1996).
- [43] M. A. Kol, A. van Dalen, A. I. P. M. de Kroon, and B. de Kruijff, *The Journal of Biological Chemistry* **278**, 24586 (2003).
- [44] D. P. Tieleman and S.-J. Marrink, *J. Am. Chem. Soc.* **128**, 12462 (2006).
- [45] A. A. Gurtovenko and I. Vattulainen, *J. Phys. Chem. B* **111**, 13554 (2007).
- [46] G. Parisio, A. Ferrarini, and M. M. Sperotto, *International Journal of Advances in Engineering Sciences and Applied Mathematics* **8**, 134 (2016).
- [47] J. S. Allhusen and J. C. Conboy, *Acc. Chem. Res.* **50**, 58 (2017).
- [48] M. H. L. Nguyen, M. DiPasquale, B. W. Rikeard, C. G. Yip, K. N. Greco, E. G. Kelley, and D. Marquardt, *New J. Chem.* **45**, 447 (2021).
- [49] P. Torriillo, A. Bogetti, and L. Chong, *J Phys Chem.* **125**, 16421649 (2021).
- [50] H. Huang, *Biochemistry* **39**, 8347 (2000).
- [51] H. Huang, F.-Y. Chen, and M.-T. Lee, *Phys Rev Lett.* **92**, 198304 (2004).

# Supplementary Information

## Translocation of a single Arg<sub>9</sub> peptide across a DOPC/DOPG(4:1) model membrane using the weighted ensemble method

Seungho Choe<sup>1,2</sup>

<sup>1</sup> *Department of Energy Science & Engineering,  
DGIST, Daegu 42988, South Korea*

<sup>2</sup> *Energy Science & Engineering Research Center,  
DGIST, Daegu 42988, South Korea*

## I. THE NUMBER OF HYDROGEN BONDS BETWEEN ARG<sub>9</sub> AND THE LIPIDS MOLECULES AND THE CONFORMATIONAL CHANGE OF ARG<sub>9</sub> DURING THE TRANSLOCATION

We counted hydrogen bonds between Arg<sub>9</sub> and the lipid molecules during the WE simulations. Fig. S1 denotes the number of hydrogen bonds calculated in VMD [1]. The blue line is the number of the hydrogen bond between Arg<sub>9</sub> and the lipids, while the green line is between Arg<sub>9</sub> and the phosphate group. On the other hand, the red line denotes the hydrogen bond between Arg<sub>9</sub> and water. Each point in the figure corresponds to an averaged value over 10 iterations. The red line shows a rapid increase when Arg<sub>9</sub> reaches the bottom of the membrane. The figure shows that the average number of hydrogen bonds between Arg<sub>9</sub> and the lipids (or water) was about 20. We suggest in the main text that the water flow and the orientation angle of Arg<sub>9</sub> are vital factors that control the translocation of Arg<sub>9</sub>.

Fig. S2 shows the conformational change of Arg<sub>9</sub>s during the WE simulation calculated in the Timeline in VMD [1]. The third Arg<sub>9</sub> is the one that showed the translocation across the membrane. The other three Arg<sub>9</sub>s showed the conformation of the random coil during the translocation, while the third one maintained “turn” conformation during the whole WE simulation.

## II. THE POTENTIAL OF MEAN FORCE(PMF) PROFILES (RAW DATA)

We have obtained five pmf profiles based on our five WE simulation data at different bin boundaries. Fig. S3 shows the raw data from each WE simulation. Next, we must combine these profiles to connect (Fig. 6 in the main text).

## III. COMPARISON OF THE ORIENTATION ANGLE OF ARG<sub>9</sub> AT THE LAST PART OF THE TRANSLOCATION

In addition to the WE5 simulation, we performed two more simulations (WE5a and WE5b) to compare the orientation angle of Arg<sub>9</sub> during the last part of the translocation to the bottom of the membrane. We used the same system set up in the WE5 simulation for the WE5a and WE5b simulations. They have the same boundary and bin size. Table S1

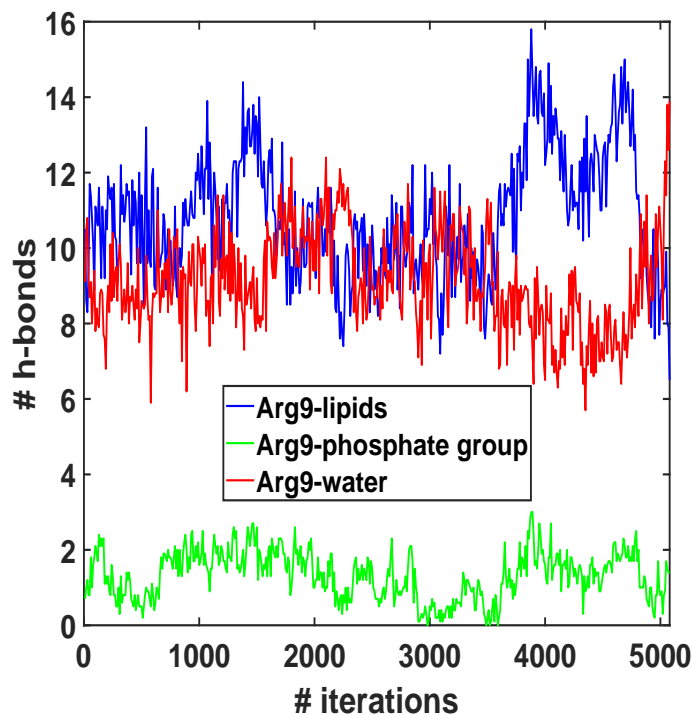


FIG. S1: The number of hydrogen bonds (blue: between Arg<sub>9</sub> and the lipids molecules, green: between Arg<sub>9</sub> and the phosphate group, red: between Arg<sub>9</sub> and water) vs. the number of iterations

denotes a list of three WE simulations performed at the end of translocation, including the WE5 simulation in the main text. Fig. S4 shows the penetration depth vs. the orientation angle from the WE5, WE5a, and WE5b simulations. The figure shows a strong correlation between the penetration depth and the orientation angle. Arg<sub>9</sub> can penetrate rapidly with a smaller orientation angle. Fig. S5 presents free energy profiles from the WE5, WE5a, and WE5b simulations and shows that a smaller angle is energetically favorable for translocating Arg<sub>9</sub> across the membrane.

#### IV. AN ADDITIONAL EQUILIBRIUM SIMULATION WITHOUT THE WE METHOD

After finishing the WE simulations (from the WE1 to WE5), we ran an additional equilibrium simulation for 1  $\mu$ s to see conformational changes of Arg<sub>9</sub>s and the lipid molecules. The equilibrium simulation method was similar to the previous ones[2, 3]. Fig. S6 presents

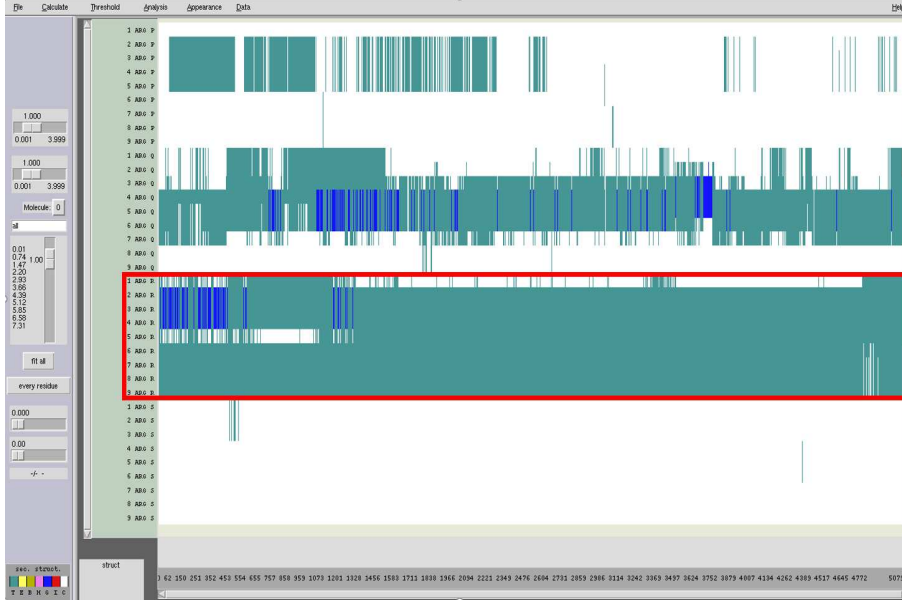


FIG. S2: The conformational change of Arg<sub>9</sub>s during the WE simulation. We used the Timeline in VMD [1]. The third Arg<sub>9</sub> is the one that showed the translocation across the membrane

TABLE S1: A list of three WE simulations performed at the last part of the translocation

simulation no.	bin boundaries	bin size (the smallest)	# iterations
WE5	$[-45.0 \text{ \AA}, -33.0 \text{ \AA}]$	$0.10 \text{ \AA}$	196
WE5a	$[-45.0 \text{ \AA}, -33.0 \text{ \AA}]$	$0.10 \text{ \AA}$	315
WE5b	$[-45.0 \text{ \AA}, -33.0 \text{ \AA}]$	$0.10 \text{ \AA}$	390

snapshots at a few different times during the equilibrium simulation. During the simulation, Arg<sub>9</sub> moved back to the membrane's middle with a few lipid molecules. As mentioned in the main text, six lipid molecules moved along with Arg<sub>9</sub> during the WE simulations. Four stayed in the lower leaflet until the end of the equilibrium simulation, while two moved back to the upper leaflet when Arg<sub>9</sub> moved back to the middle of the membrane. Since the equilibrium simulation started, it took about 45 ns for two lipids to move back to the upper leaflet. The water flow and the movement of Arg<sub>9</sub> affect the phospholipid(PL) translocation. The water pore was closed after about 70 ns, as shown in Fig. S7. Fig. S7 presents the total number of water molecules translocated across the membrane during the first 100 ns

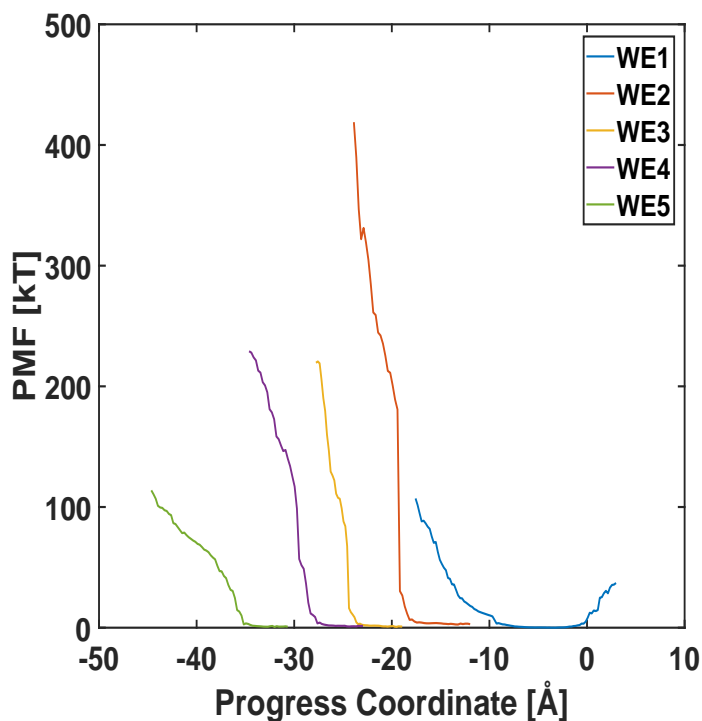


FIG. S3: Comparison of free energy profiles(raw data) along the progress coordinate.

simulation. Before closing the water pore ( $\sim 70$  ns), the upward water flux was 1.5 (water molecules/ns), while the downward water flux was 1.2. The upward water flux is slightly higher than the downward water flux due to the upward movement of Arg<sub>9</sub>.

- 
- [1] W. Humphrey, A. Dalke, and K. Schulten, *J. Molec. Graphics* **14**, 33 (1996).
  - [2] S. Choe, *AIP Advances* **10**, 105103 (2020).
  - [3] S. Choe, *Membranes* **11**, 974 (2021).

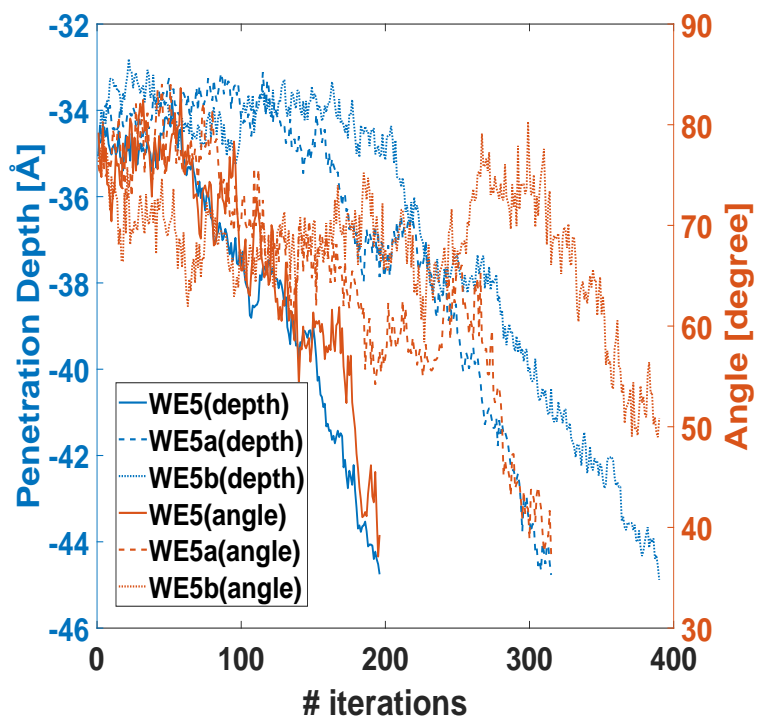


FIG. S4: The penetration depth vs. the orientation angle

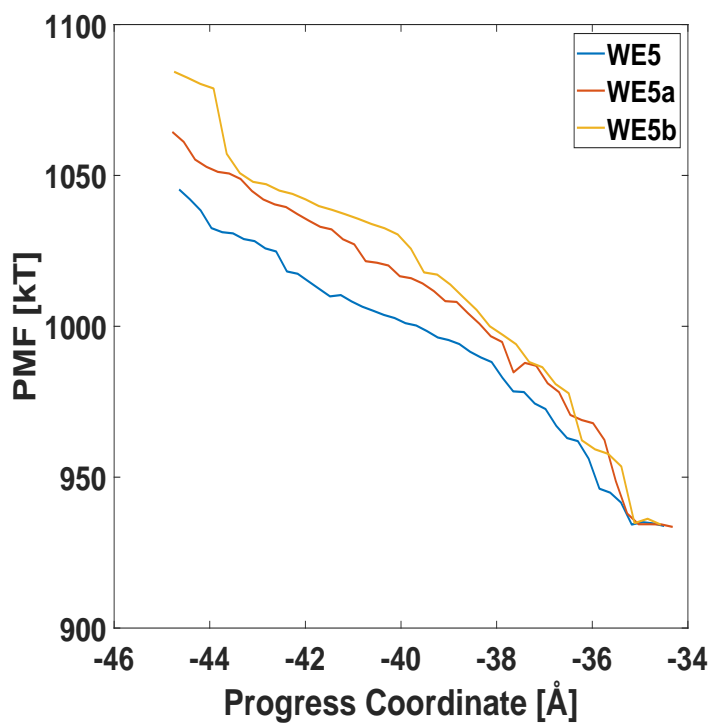


FIG. S5: Comparison of free energy between the WE5, WE5a, and WE5b simulations.

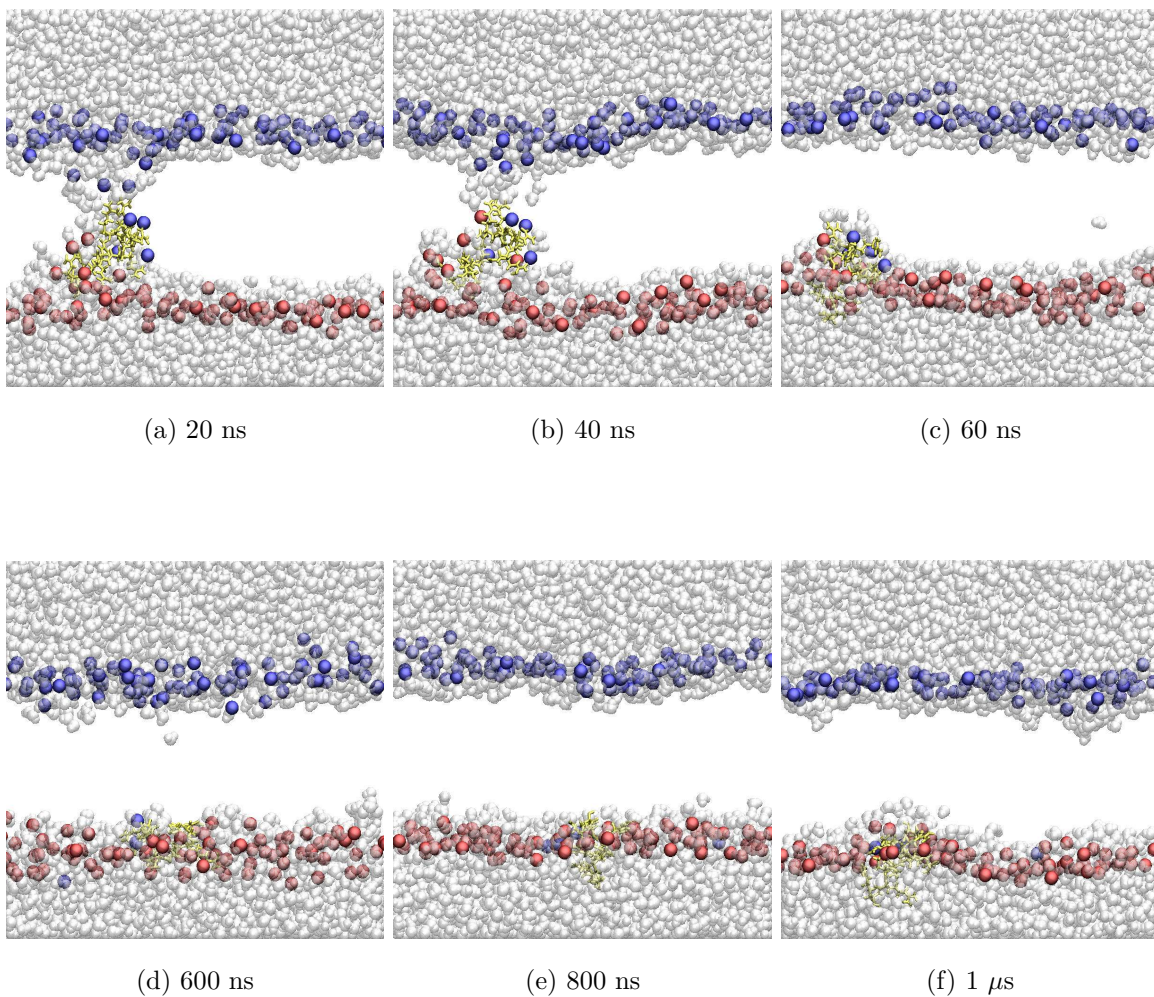


FIG. S6: Snapshots at (a) 20 ns (b) 40 ns (c) 60 ns (d) 600 ns (e) 800 ns, and (f) 1  $\mu$ s during the additional equilibrium simulation (yellow: Arg<sub>9</sub>, white: water, blue & red : phosphorus atoms of the upper leaflet & lower leaflet, respectively).

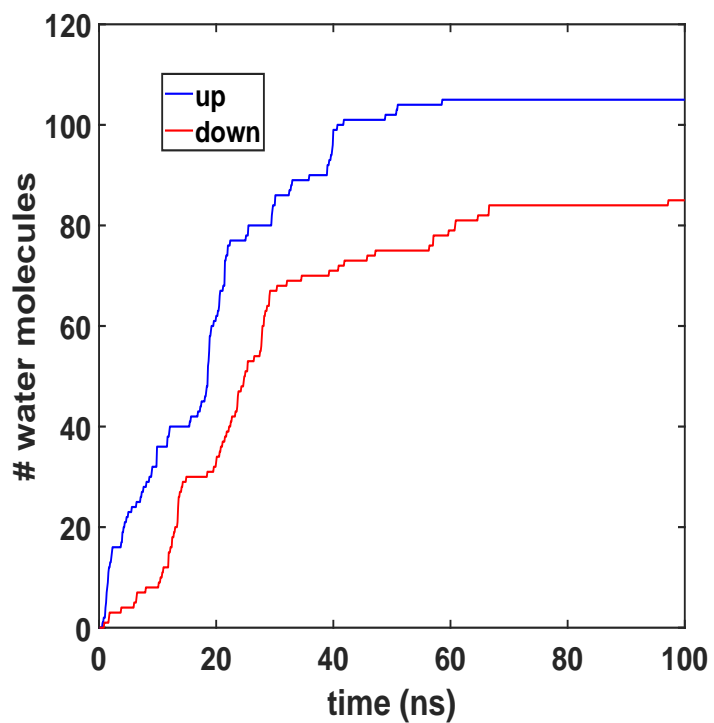


FIG. S7: A total accumulated number of water molecules translocated across the membrane (the moving-up & the moving-down) vs. equilibrium simulation time